Proceedings of GLOBAL 2011
Makuhari, Japan, Dec. 11-16, 2011
Paper No. 395793

Quartz-Crystal Spectrometer for the Analysis of Plutonium K X-Rays

Alison V. Goodsell, William S. Charlton

alisong@tamu.edu, charlton@ne.tamu.edu

Nuclear Security Science & Policy Institute

Texas A&M University, College Station, Texas, 77843-3473, USA

ABSTRACT: The ability to quickly quantify the Pu content within spent nuclear fuel (SNF) is essential to nuclear forensics. Analysis of the Pu to U ratio can provide information on fuel which could contribute to the attribution of a fuel sample. Plutonium concentration data can be acquired through non-destructive analysis (NDA) by detecting self-induced x-ray fluorescence (XRF) from Pu in the fuel. However, during conventional spectroscopy, the characteristic Pu x-ray peak of interest lies beneath background and requires an extended count time. Crystal spectrometers allow x-rays of selected energies, obeying Bragg's law for coherent scattering of incident photons, to be focused directly onto a detector. This provides a high signal with limited background by decreasing the possible Compton interaction in the detector. The crystal design and the experimental geometry that would allow for the study of high energy x-rays required further attention. In addition, a preliminary MCNP simulation of the energy-direction coupled photon source from the quartz crystal was used to calculate the improved signal-to-noise ratio of the Pu x-ray peak above background.

KEYWORDS: *x-ray fluorescence, plutonium, K x-rays, Bragg diffraction*

I. INTRODUCTION

Spent nuclear fuel (SNF) has the potential to be a major radiological threat in the hands of a terrorist group. Nuclear forensics, acting as a deterrent, requires the ability to quickly identify the origin of an interdicted material. Non-destructive gamma spectroscopy is one method to relatively quickly ascertain fuel information. Previous research investigated the detection of self-induced x-ray fluorescence (XRF) to determine the Pu to U ratio within light water reactor spent nuclear fuel [1]. However, the Compton background produced by higher energy photons scattering within the SNF, collimator and detector resulted in high background counts which significantly decreased the signal-to-noise ratio, requiring long count times (Fig. 1).

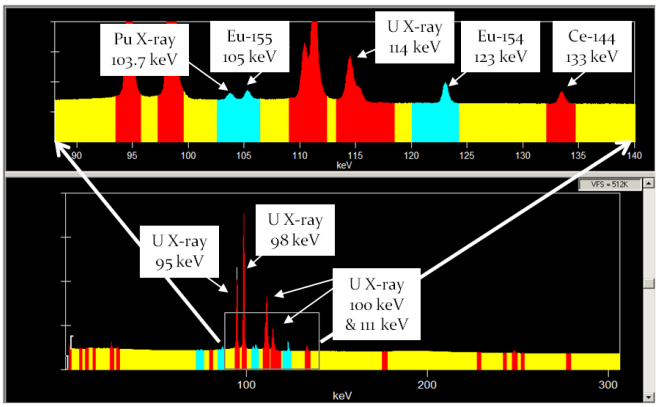

Figure 1. PWR SNF XRF 12 hour measurement showing the low signal to noise ratio at the 103.7 keV Pu XRF line (July 2008) [1]

For pressurized water reactor (PWR) SNF, Pu accounts for approximately 1% of the SNF mass, with the remaining 99% composed of U and fission products. The energy of the Pu photon of interest is relatively low at 103.7 keV, such that only the emissions at the very outward edge of the SNF survive travel to the detector without being self-attenuated. Thus, relatively few viable Pu x-rays are emitted for spectroscopy. As seen by Figure 1, the 103.7 keV Pu x-ray peak of interest is dwarfed by the surrounding peaks and is diminished by the Compton background caused by other radiation emitted from the SNF, especially the ^{137}Cs 662 keV gamma peak. These factors illustrate why a longer exposure time is required to accumulate a significant Pu peak. Methods to decrease the Compton background in the detector would lead to shorter counting times and more precise measurements.

The Pu x-ray emissions from SNF are due to self-induced XRF. These are primarily caused by gamma-ray and beta-ray emissions from the decay of fission products in the SNF. This radiation causes self-induced x-ray fluorescence of the atoms within the fuel. Figure 2 illustrates an incident gamma-ray, with energy greater than the electron shell binding energy, interacting with a tightly bound, inner K-shell electron, causing it to be ejected from the atom's electron cloud. An L-shell electron may drop into this vacancy. This electron transition is accompanied by the release of a characteristic x-ray. Each element's characteristic XRF is unique as the energy released corresponds to the difference in binding energy of the two electron shells. As seen in Table 1, Pu and U have x-ray energies ranging from 99 to 120 keV and 94 to 115 keV, respectively, depending on the electron shells involved in the transition [2]. The primary x-ray interest to this work is the 103.7 keV $K_{\alpha 1}$ x-ray from Pu, as it is the most intense.

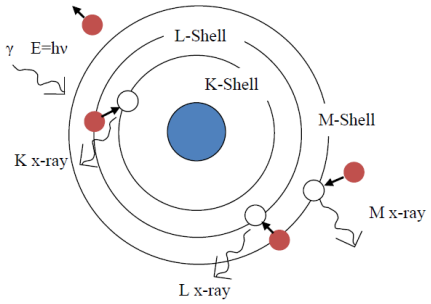

Figure 2. Simplified XRF diagram [1].

Table 1. Uranium and plutonium characteristic x-ray data [2].

X-Ray	Energy [keV]		Relative Intensity	
	Uranium	Plutonium	Uranium	Plutonium
$K_{\alpha1}$	98.44	103.76	100	100
$K_{\alpha2}$	94.67	99.55	61.9	62.5
$K_{\beta1}$	111.30	117.26	22.0	22.2
$K_{\beta2}$	114.50	120.60	12.3	12.5
$K_{\beta3}$	110.41	116.27	11.6	11.7

II. Quart-Crystal Spectrometer Design

One possible technique to increase the signal-to-noise ratio in these measurements is through the use of a crystal spectrometer. Crystal spectrometers have been used since the 1930s to obtain photon spectra by using the wave properties of light. Wavelength-dispersive spectroscopy uses a crystal of known properties to diffract x-rays according to Bragg's Law:

$$n\lambda = 2dsin\theta \quad (1)$$

where λ is the photon wavelength, d is the crystal's interplanar spacing, θ is the Bragg angle of diffraction and n is a positive integer. Thus, an array of x-ray energies and their corresponding wavelengths will each have a unique, first-order Bragg angle. This allows for a detector to be positioned specifically for the detection of a desired photon energy.

The design of the crystal spectrometer system must conform to a number of experiment-specific requirements. For the analysis of the SNF, these constraints include a stationary x-ray source, specially designed collimators, and a precisely positioned detector. The proposed dimensions of the crystal to be used for this experiment are approximately 10 cm long by 4 cm wide by 0.1 cm thick.

In this work, quartz was chosen as the crystal material since it has been used successfully in other crystal spectrometer studies [3,4]. The quartz molecule is composed of silicon and oxygen. Quartz crystals (QC) are commercially available at a relatively low cost compared to other materials and multiple private companies offer services in the construction of high-quality quartz crystals. The price depends on the required design and size of the desired crystal. Various quartz lattice structures and interplanar spacings are available for purchase. The current crystal design of interest possesses an interplanar spacing ($2d$) of 0.1624 nm.

The interplanar spacing of the crystalline lattice structure is an essential parameter of the crystal design. For Bragg x-ray diffraction, two times the spacing between the atoms must be greater than or approximately equal to the magnitude of the x-ray wavelength for a physically realistic system. Thus, to obey Bragg diffraction as described in Eq. 1, $n\lambda < 2d$ for a realistic Bragg angle. For a 103.7 keV Pu x-ray, using $E=hc/\lambda$, where E is the photon energy, h is Planck's constant and c is the speed of light, the corresponding wavelength (λ) is 0.01196 nm.

The spectrometer will operate in transmission mode using the Cauchois (or Laue) design, such that the x-rays pass completely through the crystal and are diffracted toward the detector on the opposite side. The crystal must be thin enough that the 100 keV x-rays are not majorly attenuated during their travel through the crystal. Other experiments for gamma and x-ray spectroscopy describe crystal thicknesses between 0.03 cm and 0.30 cm [3,4]. This thickness must be optimized to maximize the x-rays diffracted toward the detector but minimize absorption via the photoelectric effect and incoherent scattering by the material.

Pinhole collimators (Fig. 3) are used to direct an essentially mono-directional beam of photons onto the quartz crystal (QC). In addition, a secondary collimator after the crystal is designed such that only photons of about the desired energy pass through to the detector. The detector considered here is high-purity germanium (HPGe) as high energy resolution is needed to resolve the x-ray peaks and it could potentially be used in the field. The signal accumulated during spectroscopy is analyzed using multichannel analyzer software to determine the incident photon energies. The x-ray energies near the 103.76 keV peak of interest were analyzed using the Bragg diffraction equation. The results produced an array of Bragg angles dependent on the photon's energy, seen in Table 2.

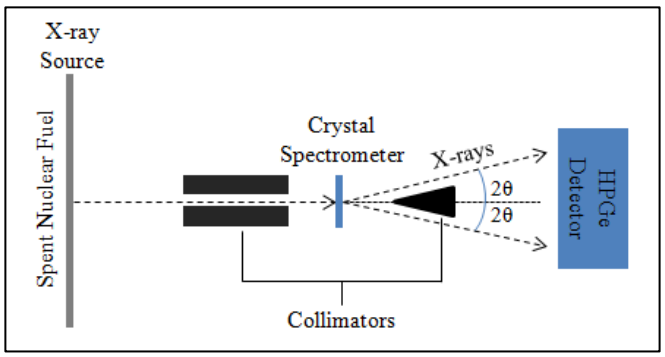

Figure 3. Basic experimental setup for transmission-mode, quartz-crystal spectrometer system.

Table 2. Energy-dependent photon diffraction through the quartz-crystal spectrometer.

Photon Source	Energy (keV)	λ (nm)	Bragg Angle θ (°)	Diffracted Angle 2θ (°)
U (XRF)	95	0.01306	4.613	9.225
U (XRF)	98	0.01266	4.471	8.942
Pu (XRF)	103.7	0.01196	4.223	8.447
Eu-155 (γ)	105	0.01182	4.174	8.348
U (XRF)	110	0.01128	3.983	7.966
U (XRF)	111	0.01118	3.947	7.895
U (XRF)	114	0.01088	3.841	7.683
Eu-154 (γ)	123	0.01009	3.562	7.124
Ce-144 (γ)	133	0.00933	3.293	6.587

Using the proposed crystal parameters, the Pu 103.7 keV x-ray of interest should be diffracted from normal by approximately 8.447°. The 105 keV gamma emission from Eu-155 should also interact with the quartz crystal lattice structure and be diffracted by 8.348° as the two photons are very close in energy. The secondary collimator radius will determine the range of x-ray energies able to interact with the HPGe detector.

III. Quartz Crystal Simulations

Using the experimental parameters and XRF data from previous research analyzing the isotopic and secondary radiation from SNF [1], the behavior of the x-rays of interest was investigated computationally. A simplified version of the SNF measurement system, including the SNF rod, the collimator, the concrete shielding and the quartz crystal, was created using MCNP, as seen in Fig. 4 [5].

The source was defined by simulating XRF within SNF using MCNP. Previous work developed the decay radiation source in the SNF via burnup simulations of Three Mile Island (TMI) PWR fuel using TRANSLAT. This SNF composition was used with MCNP to simulate the secondary radiation from Pu and other elements. The emissions from the SNF were recorded using an energy-binned surface flux tally to record the energy-dependent photon flux on the QC surface.

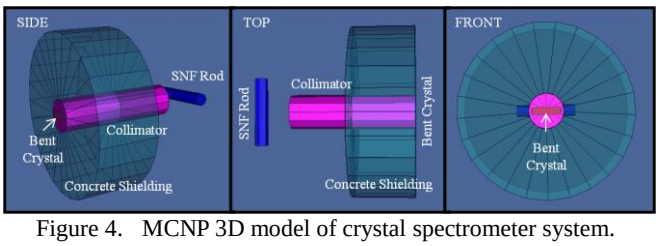

Figure 4. MCNP 3D model of crystal spectrometer system.

Due to MCNP being unable to model the wave properties of light, an external routine was used to determine each incident photon's angle of diffraction using the proposed crystal properties and Bragg's Law from Eq. 1. Each photon's angle was then changed according to Bragg's law to simulate the diffraction of these photons through the crystal. This was performed for all of the photons between 80 keV and 1.2 MeV. Lower energy photons (< 80 keV) were ignored as they would suffer from a large attenuation via the photoelectric effect while traversing the crystal and would not contribute to counts around 100 keV. This produced a final radiation source "exiting" the quartz crystal including their energy and energy-dependent direction.

It should be noted that photons with energies greater than 400 keV were diffracted by less than 2° from normal. Thus, it would be expected that photons of higher energies would pass directly through the QC without any significant attenuation via diffraction or absorption and be blocked by the secondary collimator before reaching the detector. These photons could however scatter in the crystal spectrometer and exit the crystal at an angle about 8.4°. While MCNP cannot simulate the diffraction of photons in the crystal, it can simulate the Compton scattering of photons in the crystal.

Two system geometries were modeled in MCNP to allow a determination of the crystal spectrometer's impact on the signal-to-noise ratio. The first geometry modeled included an XRF source incident on a HPGe detector without any diffraction due to a quartz crystal (Fig *5i*). The second geometry modeled included the direction-specific XRF source after being diffracted by the crystal (Fig. *5ii*). Both setups included the use of a 0.3 cm wide by 0.3 cm tall by 10 cm long collimator. For the first simulation (*i*), the radiation traveled in a straight line down the collimator onto the detector surface. In the second setup (*ii*), the energy-direction coupled radiation traveled down a collimator that had been skewed by approximately 8.4°, to allow only the photons around the 100 keV energy of interest (diffracted approximately 8.4°) to successfully travel the length of the collimator and interact with the detector crystal. For both simulations, a pulse height tally was taken in the HPGe detector cell and used to determine the signal-to-noise ratio.

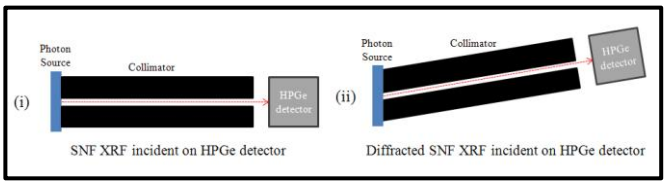

Figure 5. Two MCNP simulation setups were run to determine the quartz crystal's effect on the detected background radiation around the Pu x-ray peak of interest.

IV. CONCLUSIONS

The F8 tallies with Gaussian energy broadening for both simulations were compared to determine the crystal's effect on the signal-to-noise ratio. As seen in Fig. 6, the Pu x-ray peak of interest at 103.76 keV is visible above background for both the simulation of the radiation directly incident on the HPGe detector without diffraction and the simulation of the energy-direction coupled source due to diffraction from the crystal spectrometer.

The calculated spectra with and without a QC were analyzed using the GENIE-2000 spectrum analysis software. The net

Pu $K_{\alpha 1}$ photopeak count above background was determined for two count times (2 and 12 hours) to evaluate the effects on the percent error and signal-to-noise ratio of the measurements.

Table 3 (at the bottom of the page) shows the photopeak counts for the 103.7 keV peak, the uncertainty in those counts and the net continuum counts for both count times with and without the crystal spectrometer.

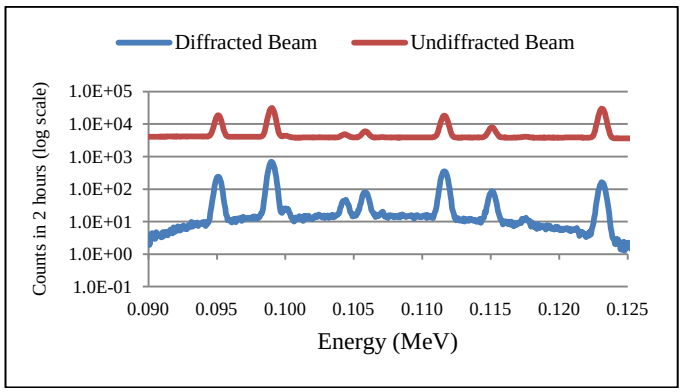

Figure 6. MCNP simulation results for the cases with and without diffraction from the quartz crystal.

Table 3 also contains an analysis of the data presented. The signal-to-noise ratio for both count times improved more than 9 times when the quartz crystal energy-direction coupling was used in the MCNP simulation. The improvement in the signal-to-noise ratio did not increase significantly with the much greater count time of 12 hours for the cases with and without the quartz crystal. Also, the ratio of percent error did not significantly decrease from approximately 3% for the longer count time. Use of the energy-direction coupled source with the crystal resulted in an order of magnitude fewer counts under the Pu 103.7 keV peak; however, this did not greatly affect the percent error as the background continuum counts were also lower. Analysis of shorter count times may be performed to determine the detection time which optimizes the signal-to-noise ratio and the percent error of the two cases. Optimization of this system would be needed to allow for a more direct comparison of the benefits of using a crystal spectrometer.

For this setup, certain assumptions were made including:

- No impurities or defects within the crystal were considered such that all photons were diffracted perfectly by the crystal spectrometer
- The collimator material is a perfect absorber though scattering due to air within the collimator tube was included
- The cold finger and dewar for the HPGe detector were neglected
- β-particle contributions to XRF are neglected as they were previously shown to be only ~20% of XRF source [1]
- The shipping tube was left on the initial SNF measurement which resulted in more scattering

The quartz-crystal spectrometer system may have the ability to decrease the required detection time for the Pu x-ray peak of interest by reducing the Compton background incident on the detector. Additional simulations shall be performed to better characterize the improved efficiency of the quartz-crystal detection system.

V. FUTURE ACTIVITIES

Future research for the quartz-crystal spectrometer for nuclear forensics applications is to (1) design and evaluate an optimized detector system, and (2) construct a more realistic simulation that better conforms to experimental requirements. Currently, an optimized collimator design is being investigated.

Once the experimental setup is confirmed and the crystal is acquired, a series of calibration and test measurements will be taken to determine the detector system's efficiency and ability to detect photon energies near the range of interest (~100 keV) and suppress Compton background due to high energy photons in the detector.

This crystal spectrometer research applies to nuclear forensics; however, there are wide ranging applications for x-ray spectroscopy using a crystal spectrometer in nuclear safeguards and disarmament.

Table 3. Data from MCNP was evaluated using Genie-2000 for the Pu $K_{\alpha 1}$ 103.7 keV peak for a simulated 2 hr and a 12 hr measurement. The signal-to-noise ratios and the measurement error with and without crystal diffraction for the Pu $K_{\alpha 1}$ 103.7 keV peak were found.

	Count Time (hr)	Photopeak (counts)	Error (counts)	Continuum (counts)	Percent Error	Signal-to-Noise Ratio	Ratio of Percent Error	Signal-to-Noise Ratio Improvement
QC	2	$2.97 \cdot 10^{2}$	24	$3.90 \cdot 10^{2}$	$7.91 \cdot 10^{-2}$	$7.62 \cdot 10^{-1}$	2.67	9.13
No QC		$87.6 \cdot 10^{2}$	260	$1050 \cdot 10^{2}$	$2.97 \cdot 10^{-2}$	$0.83 \cdot 10^{-1}$		
QC	12	$18.2 \cdot 10^{2}$	57	$24.6 \cdot 10^{2}$	$3.14 \cdot 10^{-2}$	$7.40 \cdot 10^{-1}$	2.50	9.48
No QC		$497 \cdot 10^{2}$	620	$6370 \cdot 10^{2}$	$1.25 \cdot 10^{-2}$	$0.78 \cdot 10^{-1}$		

REFERENCES

1. A.S. Stafford, "SNF Self-Induced XRF to Predict Pu to U Content," M.S. Thesis, Texas A&M University, College Station (2010).
2. D. Reilly, N. Ensslin, and H. Smith, "Passive Nondestructive Assay of Nuclear Materials," United States Nuclear Regulatory Commission, Washington, DC, NUREG/CR-5550, 1991.
3. E.O. Baranova, M.M. Stephanenko, "Cauchois-Johansson X-ray Spectrograph for 1.5 to 400 keV Energy Range," *Rev. Sci. Instr*., vol 72, no. 2, Feb 2001.
4. J.W.M. DuMond, "Gamma-Ray Spectroscopy by Direct Crystal Diffraction," *Ann. Rev. Nucl. Sci*., vol. 8, pg 163-180, 1958.
5. "MCNP – A General Monte Carlo N-Particle Transport Code Version 5 Manual," Los Alamos National Security, 2005.